

Jonas Berking – Brigitta Schütt

Geoarchaeology and Chronostratigraphy in the
Vicinity of Meroitic Naga in Northern Sudan –
A Review

Communicated by Michael Meyer

Edited by Gerd Graßhoff and Michael Meyer,
Excellence Cluster Topoi, Berlin

eTopoi ISSN 2192-2608

<http://journal.topoi.org>



Except where otherwise noted,
content is licensed under a Creative Commons
Attribution 3.0 License:

<http://creativecommons.org/licenses/by/3.0>

Jonas Berking – Brigitta Schütt

Geoarchaeology and Chronostratigraphy in the Vicinity of Meroitic Naga in Northern Sudan – A Review

Communicated by Michael Meyer

The ancient and now abandoned settlement of Naga, had its heyday around 2000 years ago, located in the hinterland of a Nile tributary. Here we present 15 new OSL-dates and four new radiocarbon-ages. Data show that fundamental environmental changes did not take place in the investigation area at least during the past 2000 years; nevertheless, subsystems may have varied significantly.

Quaternary chronology; desert margins; drylands; climatic oscillations; NE Africa; landscape reconstruction.

Im Hinterland eines Nil Tributäres bestand vor rund 2000 Jahren die, später aufgegebene, Stadt Naga. Hier präsentieren wir 15 neue OSL- und vier neue Radiokarbon-Alter. Die Ergebnisse zeigen, dass im Untersuchungsgebiet fundamentale Umweltänderungen mindestens seit den letzten 2000 Jahren nicht mehr stattfanden, sich jedoch Subsysteme signifikant geändert haben können.

Quartär-Chronologie; Wüstenränder; Trockenräume; Klimaschwankungen; NO-Afrika; Landschaftsrekonstruktion.

1 Scope of the Geoarchaeological Research at Naga

The scope of this paper is to summarize the investigations on landscape history and landscape archeology which took place between 2008 and 2010 in semi-arid northern Sudan at the excavation site of the ancient town of Naga, located about 40km south of the river Nile in the dry savannah (Fig. 1). Crucial and widely acknowledged factors of landscape evolution such as climate variability, tectonic activities and surface shaping processes as well as direct and indirect human impact were recorded and evaluated. To understand the landscape history, it is essential to establish a robust chronology, enabling a contextualization with the archaeological timeframes.¹

At least since the mid-20th century, geoarchaeological approaches, in the sense of archaeological issues analyzed and investigated by geoscientists, have become increasingly important at archaeological excavations.² Various geoscientific methods are applied to

This study is supported by the Cluster of Excellence Exc264 Topoi – The Formation and Transformation of Space and Knowledge in Ancient Civilizations – Research Area A-I-7. Special thanks go to Dietrich Wildung and Karla Kröper, “Ägyptisches Museum Berlin”; who facilitated field work, to Michael Schott and Julia Meister for assistance during fieldwork and their appraising work, and to Brian Beckers, Janina Körper, Sebastian Wagner, Burkhard Ullrich and many others for an enlightening interdisciplinary research within the pleasant setting and support of Topoi.

1 Fuchs 2006.

2 Gladfelter 1977.

answer the manifold specific questions at the particular study and excavation sites.³ At Naga, located in the semi-arid Sudan, at the southern margin of the Saharan desert, one of the major geoarchaeological questions is about the history of climate and whether the ancient cultures experienced more humid and favorable environmental conditions.⁴ In this sense, the present study analyzes the paleoenvironmental situation through the application of highly resolved, spatially differentiated modeling approaches. The incorporation of the recorded terrain data as well as the analysis of terrestrial archives and their chronology enables us to reconstruct the paleoenvironment.

However, this paper does not seek to summarize all research, results and investigations, nor to discuss the meaning of every single age determination with respect to its possible geoscientific or archaeological context, but merely to present a comprehensive review of already published interpretations.⁵

2 Introduction and State of the Art

The early Holocene African Humid Period was a period of favorable water balance, and fresh water was available in wide areas of the Sahara.⁶ Ongoing Holocene aridization caused its inhabitants to migrate into areas with a reliable water supply, predominantly along rivers and in mountain and groundwater oases. Aridization of the Sahara reached its maximum at the beginning of the Common Era.⁷

Consequently, the end of the Holocene African Humid Period in Northern Africa marked the beginning of the meteoric rise in importance of the Nile valley as a settlement area.⁸ The Egyptian society started to develop along the Nile's lower course in the fourth millennium BCE, whereas the Nubian society evolved along its middle course in several stages from the first millennium BCE onwards, toward the kingdom of Kush, located between the first and sixth cataracts (Fig. 1).

The last epoch of the kingdom of Kush is called Meroitic, attended by the move of its capital from Napata at the Fourth Nile cataract southwards to Meroe, close to the mouth of the river Atbara. There were several reasons for this move, including (i) political reasons and the kingdom's release from the Egyptian empire, but also (ii) economic reasons due to Meroe's role as a trade center with middle and southern Africa, and most likely (iii) increasing aridity causing climatic stress, forcing the population to move southward towards the Sahel, with its more reliable monsoonal rainfalls.

The city of Naga is one of the most important cities of this Meroitic epoch, located about 180km south of Meroe and about 150km north of the modern Sudanese capital, Khartoum. Along the river Nile, Naga is one of the few central places with sacral and residential functions that is not located in the direct vicinity of the Nile, but about 40km beyond, in its south-eastern hinterland.⁹ The city of Naga covered an area of at least 1.2km². The excavation revealed several constructions including temples, governance and administrative buildings as well as well-preserved cemeteries. The existence of the city of Naga dates from the fourth century BCE to the fourth century CE, with its heyday around the turn from BCE to CE.¹⁰

3 Gladfelter 1977.

4 Kuper and Kroepelin 2006.

5 Berking and Schütt 2011; Berking et al. (Forthcoming); Berking, Beckers, and Schütt 2010.

6 Pachur and Hoelzmann 2000.

7 Kuper and Kroepelin 2006.

8 Kuper and Kroepelin 2006.

9 Kröper 2006–2007.

10 Kröper 2006–2007.



Fig. 1 | A: Map of the Nile river with the modern capitals of Sudan and Egypt highlighted (Roman numbers signify the cataracts). B: Map of the study area in the hinterland of the Nile; the Wadi Awatib catchment and the location of Naga are highlighted.
J. Berking.

Today, Naga is abandoned. Temples and administrative buildings are ruined, weathered and covered by dune sands. Only few peasants or semi-nomads live in the area, raising cattle and practicing runoff-fed agriculture along the floodplain of the Wadi Awatib during the rainy season.¹¹ This setting of a formerly important but now abandoned city in a presently altogether barren environment and the question of how its inhabitants coped with aridity and the imponderability of monsoon arrival have given rise to various geoarchaeological research topics.¹²

3 Study Site

The excavation site of Naga is located at the foot of an escarpment range on the right bank of the Wadi Awatib (Fig. 2). The ephemeral character of the Wadi Awatib is determined by a regional dry savannah climate. Temperatures are high throughout the year with an annual average temperature of 29.3° C¹³ and an average precipitation of 94mm/a¹⁴. The rainy season occurs during the summer months (June–August), bringing 95 % of the total

11 Gabriel 1997.

12 Berking and Schütt 2011; Berking et al. (Forthcoming); Berking, Beckers, and Schütt 2010.

13 GLOBALSOD, 1961–1990.

14 GLOBALSOD, 1961–1990.

rainfall amount.¹⁵ During rainy seasons, high rainfall intensities periodically exceed the soil's infiltration capacity; thus *Hortonian* runoff occurs after short and heavy rainfall events along the slopes and in the receiving wadis.¹⁶

The drainage divide of the Wadi Awatib runs along the escarpment ranges which flank both sides of the riverbed and rise up to 90m above the valley bottom. The bedrock forming the escarpments is of Cretaceous sandstone belonging to the south-eastern branch of the Nubian sandstone complex¹⁷ and consists almost entirely of quartz¹⁸. During weathering processes, migration and oxidation of accessory iron minerals (Fe II → Fe III) caused a reddish to blackish color wherever the Cretaceous bedrock is exposed. Soils are mainly Leptosols along the escarpment and its pediments, where Arenosols developed in the dunes, both with a predominantly coarse sand texture. Fluvisols with a loamy texture predominate along the alluvial plain of the Wadi Awatib. Here the rise of soil water and finally its evaporation cause the formation of sub-surface silica incrustations.¹⁹

All over the study area, the occurrence of sparse, drought-resistant vegetation is controlled by climatic presetting and is modified by human impact, such as grazing or clearing. *Acacia tortilis* and *Acacia mellifera* are the most prominent trees, occurring either as riverine forests or in little patches next to the riverbeds associated with *Astrebla s.* and *Panicum turgidum*.²⁰ Whereas the middle and lower courses of Wadi Awatib show the typical contracted vegetation pattern of drylands, a dense dry-savannah vegetation occurs in the remote areas of the upper course.²¹

A salient feature throughout the geoarchaeological investigations is the aforementioned ephemeral character of available precipitation and hence available water. The Meroitic engineers adapted to the dry season and the periodic precipitation and runoff events by constructing an open water reservoir called hafir (Arabic: *dig*). Hafirs are hand-dug depressions, encircled by walls built of the excavated material. The use of small hafirs is still common in the area at the present time, their water being predominantly used for irrigation and for cattle farming. The Meroitic reservoir known as the "Great Hafir of Naga" is located at the right river bank of Wadi Awatib about 0.5km upstream of the city of Naga, at the confluence of a minor tributary.²² Its construction dates back to Meroitic times; at present it is inactive due to siltation processes.²³ More hafirs from the Meroitic phase are found in Musawwarat es Sufra about 30km northeast of Naga.²⁴

4 Synopsis of the Applied Methods and Materials

4.1 Field Work

During field work geomorphological mapping was supported by a Differential Global Positioning System (DGPS). Landforms and topography were systematically recorded. Transects from the escarpment areas into the wadis were measured along with the recording of landforms. Colluvial, eolian and alluvial sediments were systematically described and sampled. Data from DGPS, field, tachymetric, remote sensing and radiometric surveys were compiled using ESRI ArcGIS (Tab. 1). To obtain paleoenvironmental proxies,

15 Berking and Schütt 2011.

16 Berking et al. (Forthcoming).

17 Klitzsch 1970.

18 Bussert 1998.

19 Zech and Hintermeier-Erhard 2002.

20 Aktar-Schuster and Mensching 1993.

21 Berking et al. (Forthcoming).

22 Berking et al. (Forthcoming).

23 Kleinschroth 1984; Kleinschroth 1986; Hinkel 1991.

24 Scheibner 2004.

	Count	Analysis / Aim / Affiliation	Published
Remote Sensing Data		High resolved RGB, NIR Data from IKONOS and ASTER satellite imagery and radiometric data from SRTM 3 mission.	1, 2, 3
Terrain Model		Several thousand DGPS measurements and tachymetry survey data lead to a terrain model of 1x1 m cell size.	2
Climatic and Hydrological Data		75 available Sudanese weather stations were evaluated.	1
Palaeoclimatic data		Time slices and downscaling experiments for climatic reconstructions were conducted.	<i>in prep.</i>
Hydrological data		A runoff model was generated through HEC HMS.	3
Groundwater samples	5	Groundwater samples were analyzed for geochemical parameters to evaluate fossil origin ⁴ .	<i>unpublished</i>
Geomorphological Mapping		The whole study site was geomorphologically mapped, with detailed investigations around the excavation site.	1
Tectonic Activity	3	Cosmogenic dating of ¹⁰ Be on quartzite was conducted on several fault lines to check on tectonic activity ² .	1*
Geophysical Prospections		Ground penetrating radar and geoelectrical surveys were conducted mainly in the surroundings of the Great Hafir.	2
Chronostratigraphy			
Sediment samples	336	Standard methods for geochemical and mineralogical treatment.* 1 Sum parameters and in several cases check on Fe _d /Fe _o -, Si-phases; grain size and microscopic analysis. ^{1/2/4/5}	1, 2*
Tube drillings	5	see above	
Archives	49	Total number of investigated archives including all inspected outcrops and drillings.	1/2/3*
¹⁴ C ages	5	Conventional radiocarbon dating on different materials ⁴ .	
OSL ages	23	Luminescence dating on eolian quartz samples (SIR Protocol) ^{3/6} .	

Tab. 1 | Overview of applied methods, specific techniques, their frequency, and the corresponding publication or affiliation. For reasons of clarity the publications are abbreviated and refer to: ¹ Berking and Schütt 2011; ² Berking et al. (Forthcoming); ³ Berking, Beckers, and Schütt 2010; “*” partly published; “1...6” in the Laboratory of (1) Physical Geography, Berlin; (2) Purdue Rare Isotope Measurement Laboratory, Indiana; (3) LIAG Institute, Hannover, (4) Department of Soil Science, TU Berlin, (5) GFZ, Potsdam (6) RLAHA Laboratory, Oxford.

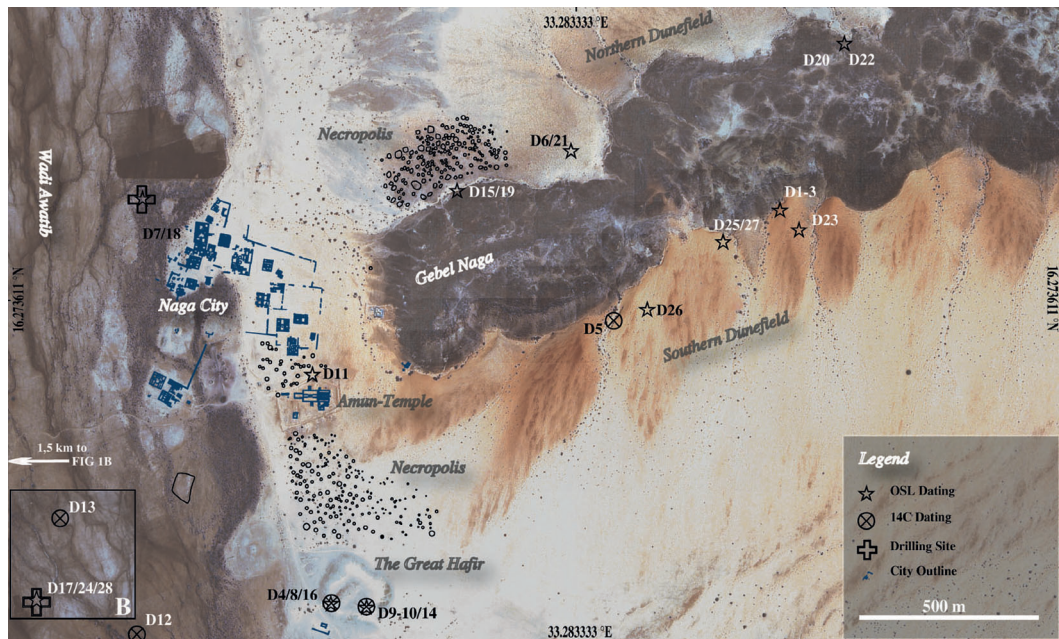


Fig. 2 | Detailed map of the study site with the location of the sampling points for the drillings and dating locations. Note that the samples codes D1,2,3... are arranged in order from D1 (youngest) to D28 (oldest) age. J. Berking.

undisturbed sediment cores were taken along a transect across the Wadi Awatib using a percussion corer. Additional sediment profiles were recorded along the river banks of Wadi Awatib and its tributaries. All sediment profiles were systematically described and sampled (Fig. 2).

4.2 OSL Dating

Mineral luminescence is the light emitted from mineral particles when they are stimulated with heat (thermoluminescence = TL) or light (optically stimulated luminescence = OSL) after receiving a dose of natural or artificial radiation. It is therefore a form of geochronology that measures the time since the last exposure of a mineral to sunlight or intense heat. A recent comprehensive review of OSL dating is given in Lian & Roberts.²⁵

The present study establishes a preliminary chronological frame for the different Quaternary relief-forming phases of the Naga site (Tab. 3 –Tab. 5). Dose rates for all samples were calculated from potassium, uranium and thorium contents measured by gamma spectrometry in the *Leibniz-Institut für Angewandte Geophysik*, Hannover (LIAG). All OSL samples were pretreated with standard methods for single-aliquot regenerative-dose protocol (SAR) at the laboratories of the LIAG. The calculated age estimates are all based on a mean water content of $3 \pm 3\%$ for all the samples, as expected from an arid depositional environment.²⁶

Aliquots were prepared from each sample under controlled laboratory lighting at the Research Laboratory for Archaeology and the History of Art, University of Oxford, by mounting small amounts of quartz grains with silicon oil onto aluminum discs. The De measurements are based on the weighted mean of twelve replicate measurements

²⁵ Lian and Roberts 2006.

²⁶ Eriksson, Olley, and Payton 2000.

performed on 4–5mm size aliquots of coarse-grained quartz (100–200 μm) using a single-aliquot regenerative-dose measurement protocol as described in Murray and Wintle.²⁷ Rejection criteria are applied according to Wintle and Murray.²⁸

All datasets assembled from field work and lab work are summarized in table 1. In-depth information about the treatments, measurements and methods applied are specified in the corresponding publications (and citations herein). The following OSL-ages are in years before present “a BP” and Radiocarbon-ages were calibrated according to Stuiver et al.²⁹ and rechecked with CalPal_{online}.

5 Chronostratigraphy

5.1 Process Domains

The study site is characterized by the typical landforms of the semi-arid, sub-Saharan landscapes. The relief is dominated by the contrasting steep slopes of the escarpment areas, accompanied by some outliers, rising several decameters above the valley bottom. At the foothills of the escarpment and its outliers, an erosional zone—*pediment*—was formed by running water, where a thin layer of pebbles overlies the bedrock.³⁰ Continuing downslope, following the gentle slope into the valleys, the pebble layer becomes thicker due to the downslope-decreasing runoff in arid areas and the high evaporation rates; consequently, it increasingly resembles an accumulation body—interpreted as *glacis*.³¹ These *glacis* merge with the floodplain where it is locally undercut by ephemeral streams. Locally, the occurrence of slump zones and landslide deposits along the steep slopes of the escarpment and its outliers point to temporarily significantly wetter environmental conditions than at present.³² In the north and south of the escarpment, corresponding to the main wind directions, the windward side (luv) and the leeward side (lee), wind-blown sands cover wide areas of the slopes and their foothills.

Direct human impact on the landscape occurs predominantly by floodwater harvesting measures—implemented as *hafirs* in the floodplain or along the slopes and as earth benches in the alluvial plain—to support infiltration by creating a slackwater environment.

Therefore four significant active or inactive process domains are distinguished. The domains are (i) eolian, (ii) fluvial, (iii) gravitational and (iv) human activity. These four process domains represent the main constituents of the dynamic landscape and hence serve as potential archives for its analysis and interpretation.

5.2 Eolian Activity

Eolian deposits cover most of the footslopes of the escarpments and their outliers along the north-facing (windward) side and the south-facing (leeward) side. Eolian deposits mostly occur as echo dunes in the slipstream and are locally covered by pebbles or gravels. The dune colors range from bright yellow to brownish-red. Linear and extensive sheet flood events probably led to incisions and encrusted zones within the dunes. Eolian activity is evident in extended dune complexes covering both sides of Gebel Naga. Owing

27 Murray and Wintle 2000.

28 Wintle and Murray 2006.

29 Stuiver, Reimer, and Braziunas 1998.

30 Berking and Schütt 2011.

31 Berking and Schütt 2011.

32 Grunert 1979.

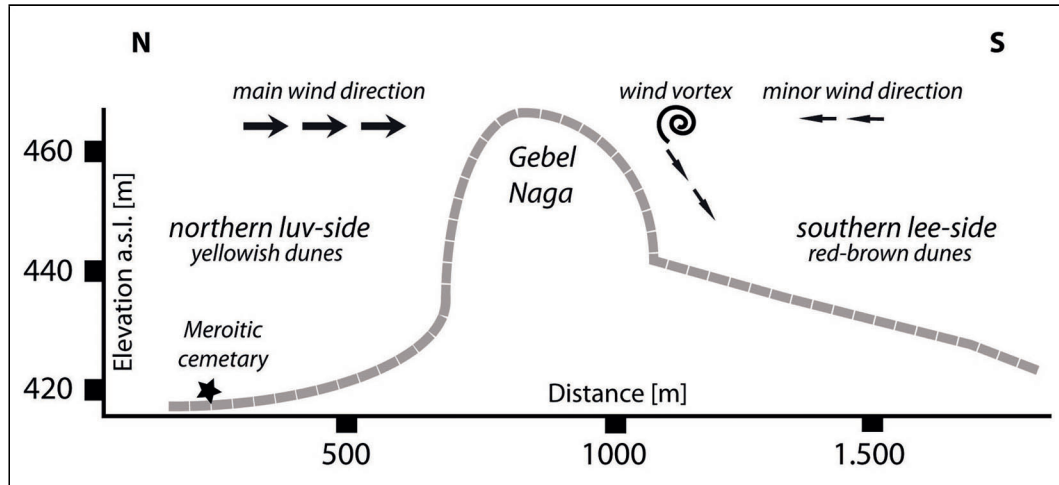


Fig. 3 | Representative topographic cross-section along Gebel Naga. The main wind direction for eight months of the year is from NNE; minor wind directions from SSW are recorded from June to September. J. Berking.

to the prevailing northerly wind direction, luv dunes evolved on the north-facing slopes of the mesa, while lee dunes occur on the southern side (Fig. 3).

The windward dunes on the northern side are predominantly yellowish in color, while the leeward dunes on the southern side are red-brown. All the investigated dunes consist of medium to fine quartz sands and show infiltration capacities of $K_s > 200 \text{ mm h}^{-1}$.³³

Luminescence and radiocarbon analysis reveals a wide range of ages for the eolian deposits from the youngest age of several decades to mid-Pleistocene ages (Tab. 2).

5.3 Fluvial Activity

The morphodynamics of Wadi Awatib are primarily controlled by the availability of water and sediments.³⁴ At present, drainage is periodic, triggered by monsoonal rainfall.³⁵ Owing to sand abundance and high flow velocity during storm-event-induced floods, the channel has an anastomizing character with a wide strath and multiple thalwegs divided by vegetated stabilized islands within subparallel banks.³⁶ Periodic floods and drying-up of the channel cause alternating erosion and accumulation processes which correspond to the character of the channel.³⁷

The alluvial plain of the Wadi Awatib with its anastomizing channels is up to 5km wide. The channels are between several centimeters and 6m deep, incised into the alluvial plain, and are often followed by a riverine forest. Signs of human activity include earth benches and fields for agricultural purposes.

Two borehole locations were chosen and revealed undisturbed alluvial sediments. The first is at $16.1068^\circ \text{ N } 33.2705^\circ \text{ E}$ at the right bank of the alluvial plain, about 150m away from the excavation site, and was sunk to a depth of 135cm. It comprises four major sections:

I (0–5cm): The topmost layer consists of bright brown, well-sorted fine sands. II (5–90cm): The main part of the core is characterized by dark brown and poorly sorted loamy

33 Berking and Schütt 2011.

34 Gabriel 1997.

35 Pflaumbaum, Pörtge, and Mensching 1990.

36 Morisawa 1968.

37 Leopold, Wolman, and Miller 1964; Morisawa 1968.

ID	Age ($\pm\sigma$)	MIS	Depth	Location
D1	59.2 \pm 15.2 a	MIS 1	45cm	<i>Dune at the</i>
D2	72.8 \pm 42.7 a	MIS 1	90cm	<i>windward</i>
D3	193.9 \pm 105.9 a	MIS 1	115cm	<i>(north-facing)</i>
D23	21.0 \pm 3.6 ka	MIS 2	15cm	<i>slope of the</i>
D26	37.7 \pm 5.3 ka	MIS 3	25cm	<i>escarpment</i>
D6	0.5 \pm 0.1 ka	MIS 1	12cm	<i>Dune at the</i>
D19	7.1 \pm 0.7 ka	MIS 1	15cm	<i>leeward</i>
D20	9.9 \pm 0.8 ka	MIS 1	100cm	<i>(south-facing)</i>
D21	10.1 \pm 1.5 ka	MIS 1	32cm	<i>slope of the</i>
D22	14.7 \pm 1.6 ka	MIS 2	130cm	<i>escarpment</i>

Tab. 2 | Age determinations along the southern and northern dune complexes of Gebel Naga.

sand, revealing the young age of 486.0 ± 49.8 a (D7, 55cm) at its center. III (90–95cm): A small horizon of fine gravel ($\emptyset < 1$ cm) embedded in a sandy matrix marks the transition to the lowest part. IV (95–135cm): The sediments consist of a bright brown, very compacted fine sand layer, yielding the relatively old age of 6.42 ± 0.45 ka (D18, 120cm).

The second drilling is located at 16.2635° N, 33.2549° E at the center of the alluvial plain and was sunk to a depth of 590cm revealing 5 major sections:

I (0–3cm): The top layer again consists of bright brown, well-sorted fine sands. II (3–80cm): Underlying sediments consist of dark brown fine sand with gravels ($\emptyset < 2$ cm) embedded in a sandy matrix, yielding the relatively old age of 5.19 ± 0.40 ka (D17, 53cm) at its center. III (80–140cm): A dark brown and highly compacted zone of loamy sand. IV (140–390cm) Dark brown fine sands, showing variations in color due to pellicles and lenses of iron and manganese dated to 1.41 ± 1.32 ka (D24, 185cm). V (390–590cm): The last section of the core is characterized by the appearance of white calcite aggregations ($\emptyset \leq 5$ cm) and a variety of colors between bright brown and orange yielding the old age of 124.07 ± 8.99 ka (D28, 587cm).

5.4 Gravitational Activity

Rotational landslides occur along the southern slope of Gebel Naga. Landslide deposits can be found at the basis of the middle slope. Poorly sorted, sharp-edged pebbles with diameters up to 12cm are embedded in a reddish, highly compacted sandy matrix. They are locally covered by slope debris and by a thin eolian sand sheet. Landslide deposits were sampled close to the western edge of Gebel Naga (16.7275° N, 33.28698° E). Resulting luminescence ages are inverted, with sample D25 dating back into MIS 3 (36.24 ± 2.62 ka; 62cm depth) and sample D27 dating back into MIS 5 (77.08 ± 5.38 ka; 14cm depth).

5.5 Human Activity

The Great Hafir of Naga was built presumably within the first centuries BCE.³⁸ The nowadays inactive and silted-up basin was sampled along two trenches and also surveyed geophysically.³⁹ The combined sedimentological and geophysical survey allowed the

38 Kleinschroth 1986.

39 Berking et al. (Forthcoming).

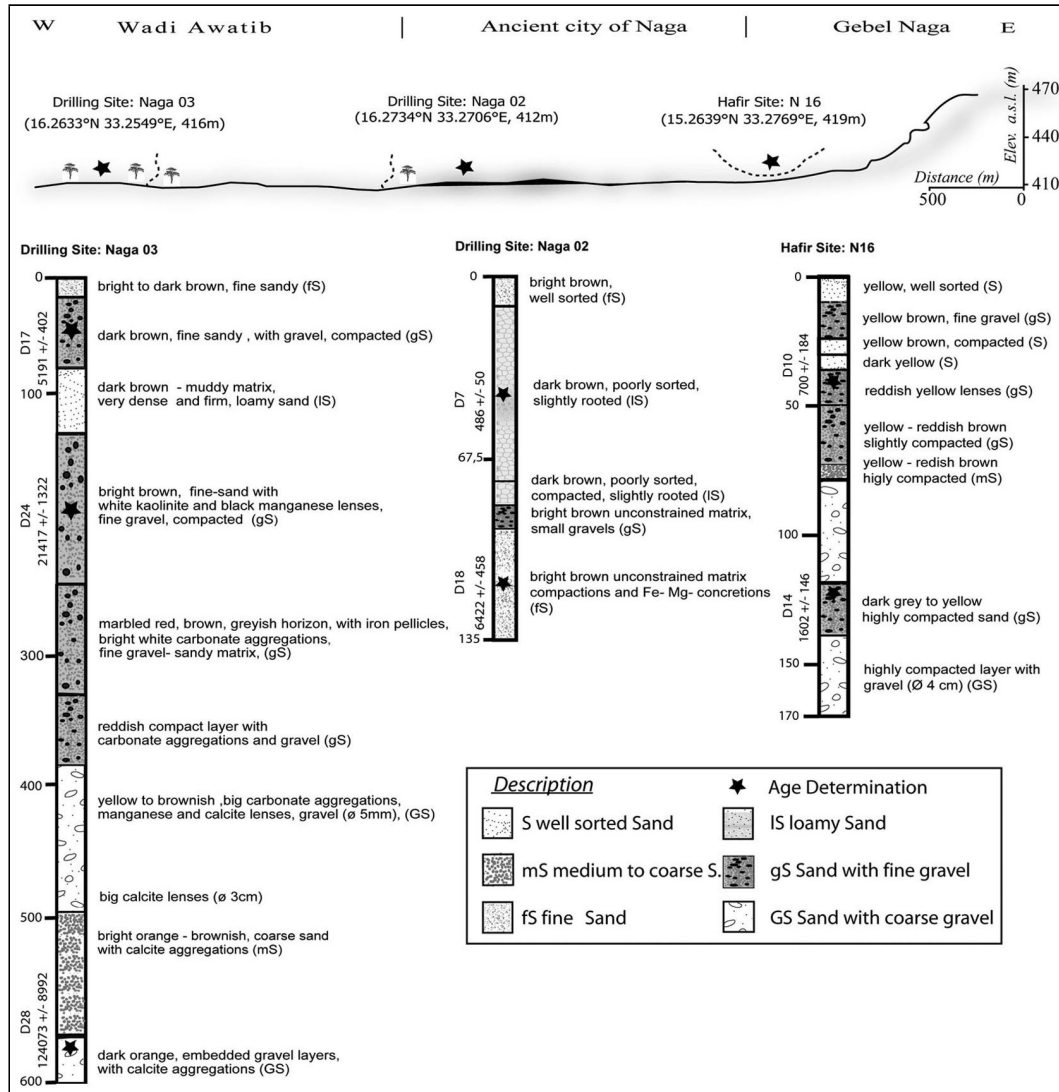


Fig. 4 | The local scale contextualization. The upper part shows a topographic cross-section from Gebel Naga into its foreland via the city, including the position of the Hafir trench and the drilling sites of Naga02 and Naga03. In the lower part the corresponding sedimentological profiles, age determinations and the corresponding depth (in cm) are shown. J. Berking.

reconstruction of the former basin, its exact location and the perception of the former reservoir (in average 9m deep) with a volume of $37,000\text{m}^3$.⁴⁰ All but one of the ^{14}C ages (D16) point to post-Meroitic siltation processes (Tab. 3).

The sample D15 was extracted from the underlying stratum of the cemetery about 250m northeast of the excavation site and yielded an age of 1.95 ± 0.64 ka at 5cm depth. Additional sediment samples were taken directly from the excavation site. The Amun temple was covered by eolian sediments until it was excavated during the past decades. The sample D11 was extracted from the eolian strata directly overlying the pediment on which the Amun temple was constructed. The pediment was reached at 45cm depth; the sediment of the overlying stratum dates to 998.0 ± 93.0 (sample D11; 16.26900° N, 33.27500° E).

40 Berking et al. (Forthcoming).

ID	Age ($\pm\sigma$)	Depth	Location
D4 (OSL age)	261.2 \pm 17.3 a	40cm	Trench near the outlet at 16.26400° N 33.27700° E
D8 (OSL)	599.2 \pm 101.2 a	85cm	Trench near the outlet at 16.26400° N 33.27700° E
D9 (cal. radiocarbon age)	695.0 \pm 25.0 a	86cm	Trench near the inlet at 16.26346° N 33.27758° E
D10 (OSL)	700.8 \pm 184.1 a	40cm	Trench near the inlet at 16.26346° N 33.27758° E
D16 (cal. radiocarbon age)	5.2 \pm 0.3 ka	100cm	Trench near the inlet at 16.26346° N 33.27758° E

Tab. 3 | Age determinations at the two trenches in the “Great Hafir basin”.

Along the foothill of Gebel Naga’s northern slope, extended tombs can be found, constructed as stone piles on top of the underlying fluvial and eolian sand. These underlying strata were sampled (D15; 16.27400° N 33.28000° E) and dated to 1.95 ± 0.64 ka at 5cm depth below the grave.

6 Contextualization and Perspectives

6.1 The Regional Timeframe

OSL dating of mostly airborne sands and radiocarbon dating mainly of charcoal pieces yielded predominantly Holocene ages ($n = 21$), some Weichselian ages ($n = 6$), and one Eemian age. Dune formation is often related to dry phases or might in historical time indicate human impact on the natural environment in the meaning of desertification processes, whereas the occurrence of alluvial, fluvial or mass movement deposits often points to wet phases.⁴¹ In this respect, chronostratigraphical information from Naga is compared with the regional and supra-regional contexts and cultural phases.

The Saharan and sub-Saharan regions experienced several dry and wet phases during the late Quaternary.⁴² During the Last Glacial Maximum, extreme aridity characterized wide areas of the Sahara and the southward adjoining Sahel, evidenced by extended dune fields deposited in the now sub-humid regions.⁴³ After the Last Glacial Maximum and the changeover to the Holocene, arid phases were repeatedly interrupted by phases of more humid conditions.⁴⁴ With the onset of the Holocene, the African Humid Period, peaking at about 8 ka, dominated environmental conditions in northern Africa.⁴⁵ During this predominantly humid phase, favorable water-balance conditions existed between 8 and 5 ka cal. BP.⁴⁶ The African Humid Period deteriorated into a continuing aridization, interrupted by phases of reduced aridization or even temporarily more humid environmental conditions.⁴⁷ The age determinations available for Naga in both long and short timeframes hardly reflect the pattern of those phases of supra-regional environmental changes, nor do they correlate with the summer insolation at 15° N, which is one of the main

41 Nicoll 2004.

42 Hoelzmann et al. 2004.

43 Hoelzmann et al. 2004.

44 Kuper and Kroepelin 2006.

45 Kuper and Kroepelin 2006.

46 Schütt and Krause 2009.

47 Pachur and Hoelzmann 2000.

Type	LUM/ HV	x °E	y °N	z m (a.s.l.)	Depth cm	Depth dev. (±) cm	Field ID	Map ID	Material	Archive	Age a	Error a	Stage MIS	published in*
OSL	1621	33.28851	16.27350	461	45		P12	D1	sand	dune 1	59.1	15.2	1	1
OSL	1622	33.28851	16.27350	461	90		P13	D2	sand	dune 1	72.8	42.7	1	1
OSL	1623	33.28851	16.27350	461	115		P14	D3	sand	dune 1	193.9	105.9	1	1
OSL	1861	33.27700	16.26400	419	40	5	OSL 27	D4	sand	alluvial (hafr)	261.2	17.3	1	
14C	25998	33.28412	16.27070	455	30	15	n 4-4	D5	coprolit	dune 2	442.0	107.0	1	
OSL	1858	33.28300	16.27500	445	12	2	OSL 14	D6	sand	dune 3	459.6	90.3	1	
OSL	1611	33.27057	16.10683	412	55	5	Naga 02-01	D7	sand	alluvial (drilling)	486.0	49.8	1	1
OSL	1862	33.27700	16.26400	419	85	3.5	OSL 28	D8	sand	alluvial (hafr)	599.2	101.2	1	
14C	25821	33.27758	16.26346	418	86	43	OSL1	D9	charcoal	alluvial (hafr)	695.0	25.0	1	2
OSL	1624	33.27758	16.26346	418	40		OSL 1	D10	sand	alluvial (hafr)	700.8	184.1	1	2
OSL	2006	33.27500	16.26900	422	45	2.5	OSL 24	D11	sand	anthropogenic	998.0	93.0	1	
14C	26000	33.27262	16.24642	418	60	30	N 20	D12	charcoal	alluvial	1026.0	164.0	1	
14C	25822	33.25600	16.26800	415	48	24	PO2_w	D13	charcoal	alluvial	1158.0	94.0	1	
OSL	2003	33.27758	16.26347	416	120	2.5	OSL 22-1	D14	sand	alluvial (hafr)	1601.6	145.7	1	
OSL	1856	33.28000	16.27400	429	5	2.5	OSL 9	D15	sand	dune (cemetary)	1952.8	646.3	1	
14C	25997	33.27668	16.26359	419	100	50	n 17	D16	charcoal	alluvial (hafr)	5155.0	273.0	1	
OSL	1613	33.25498	16.26350	416	53	6	Naga 03-01	D17	sand	alluvial (drilling)	5191.5	402.0	1	
OSL	1612	33.27057	16.10683	412	120	4	Naga 02-02	D18	sand	alluvial (drilling)	6421.7	458.3	1	1
OSL	1857	33.28000	16.27400	429	15	2.5	OSL 10	D19	sand	dune 4	7077.5	708.7	1	
OSL	2005	33.29021	16.27771	464	100		OSL 23-1	D20	sand	dune 5	9926.8	809.2	1	
OSL	1859	33.28300	16.27500	445	32	2	OSL 15	D21	sand	dune 6	10130.0	1509.2	1	
OSL	2004	33.29021	16.27771	464	130		OSL 22-2	D22	sand	dune 7	14727.3	1602.4	2	
OSL	1860	33.28900	16.27300	466	15	2.5	OSL 20	D23	sand	dune 1	21049.2	3556.6	2	
OSL	1615	33.25498	16.26350	416	185	5	Naga 03-03	D24	sand	alluvial (drilling)	21417.6	1322.7	2	
OSL	1620	33.28698	16.27275	459	62	1	P11	D25	sand	mass movment	36243.3	2628.6	3	1
OSL	1855	33.28500	16.27100	461	25	2.5	OSL 3	D26	sand	dune 2	37749.7	5256.4	3	
OSL	1619	33.28698	16.27275	459	14	1	P10	D27	sand	mass movment	77087.9	5382.0	5	1
OSL	1618	33.25498	16.26350	416	587	6	Naga 03-08	D28	sand	alluvial (drilling)	124073.6	8992.9	5e	

Tab. 4 | Compilation of the age determinations. The abbreviations for publications are identical to those in Table 1.

Map ID	Field name	Sample code	Lab No.	Lat E	Long N	Altitude [m a.s.l.]	% K	% K error	ppm Th	ppm Th error	ppm U	ppm U error	Dose rate, Gy/ka	Dose rate error	Mean recycling ratio	Mean thermal transfer [%]	Mean IRSL/OSL ratio
D1	P12	1621	X3398	33.28851	16.27350	461	0.13	0.013	2.67	0.04	0.76	0.03	0.68	0.04	1.06	10.57	0.426
D2	P13	1622	X3399	33.28851	16.27350	461	0.08	0.008	1.62	0.04	0.59	0.02	0.51	0.02	—	—	—
D3	P14	1623	X3400	33.28851	16.27350	461	0.09	0.009	2.19	0.03	0.73	0.02	0.58	0.03	0.95	—	—
D4	OSL 27	1861	X3774	33.27700	16.26400	419	0.25	0.01	2.27	0.03	1.60	0.02	0.20	0.00	—	—	—
D6	OSL 14	1858	X3771	33.28412	16.27070	445	0.20	0.01	1.95	0.12	1.21	0.13	0.21	0.00	—	—	—
D7	Naga 02-01	1611	X3388	33.28300	16.27500	412	0.5	0.05	4.41	0.08	1.25	0.04	1.26	0.07	1.07	2.76	0.007
D8	OSL 28	1862	X3775	33.27057	16.10683	419	0.19	0.01	1.61	0.02	0.62	0.01	0.19	0.00	—	—	—
D10	OSL 1	1624	X3401	33.27758	16.26346	418	0.05	0.005	0.85	0.04	0.42	0.02	0.40	0.03	1.02	—	—
D11	OSL 24	2006	X3559	33.27500	16.26900	422	0.26	0.01	2.41	0.03	0.84	0.16	0.20	0.00	—	—	—
D14	OSL 22-1	2003	X3856	33.27758	16.26347	416	0.04	0.01	1.89	0.02	0.64	0.01	0.18	0.00	—	—	—
D15	OSL 9	1856	X3769	33.28000	16.27400	429	0.11	0.01	2.79	0.04	0.88	0.02	0.21	0.00	—	—	—
D17	Naga 03-01	1613	X3390	33.25498	16.26350	416	0.46	0.046	4.5	0.05	1.21	0.02	1.22	0.07	1.06	0.83	0.0006
D18	Naga 02-02	1612	X3389	33.27057	16.10683	412	0.51	0.051	4.31	0.06	1.27	0.04	1.26	0.07	1.06	1.21	0.0007
D19	OSL 10	1857	X3770	33.28000	16.27400	429	0.09	0.01	2.58	0.04	0.93	0.02	0.21	0.00	—	—	—
D20	OSL 23-1	2005	X3858	33.29021	16.27771	464	0.31	0.01	2.35	0.30	1.02	0.24	0.18	0.00	—	—	—
D21	OSL 15	1859	X3772	33.28300	16.27500	445	0.08	0.01	1.63	0.03	1.07	0.01	0.20	0.00	—	—	—
D22	OSL 22-2	2004	X3857	33.29021	16.27771	464	0.34	0.01	1.88	0.03	0.74	0.02	0.18	0.00	—	—	—
D23	OSL 20	1860	X3773	33.28900	16.27300	466	0.19	0.01	2.32	0.58	1.44	0.22	0.21	0.00	—	—	—
D24	Naga 03-03	1615	X3392	33.25498	16.26350	416	0.35	0.035	3.41	0.05	1.07	0.02	1.00	0.05	1.02	—	0.0009
D25	P11	1620	X3397	33.28698	16.27275	459	0.09	0.009	2.17	0.05	0.72	0.02	0.59	0.03	1.4	1.3	0.0004
D26	OSL 3	1855	X3768	33.28500	16.27100	461	0.12	0.01	2.51	0.04	0.74	0.02	0.20	0.00	—	—	—
D27	P10	1619	X3396	33.28698	16.27275	459	0.11	0.011	2.39	0.05	0.81	0.02	0.66	0.03	—	—	0.0007
D28	Naga 03-08	1618	X3395	33.25498	16.26350	416	0.12	0.012	1.89	0.04	0.62	0.02	0.57	0.03	0.99	0.29	0.001

Tab. 5 | Details for the age determination. A: OSL Details. B: ¹⁴C Details.

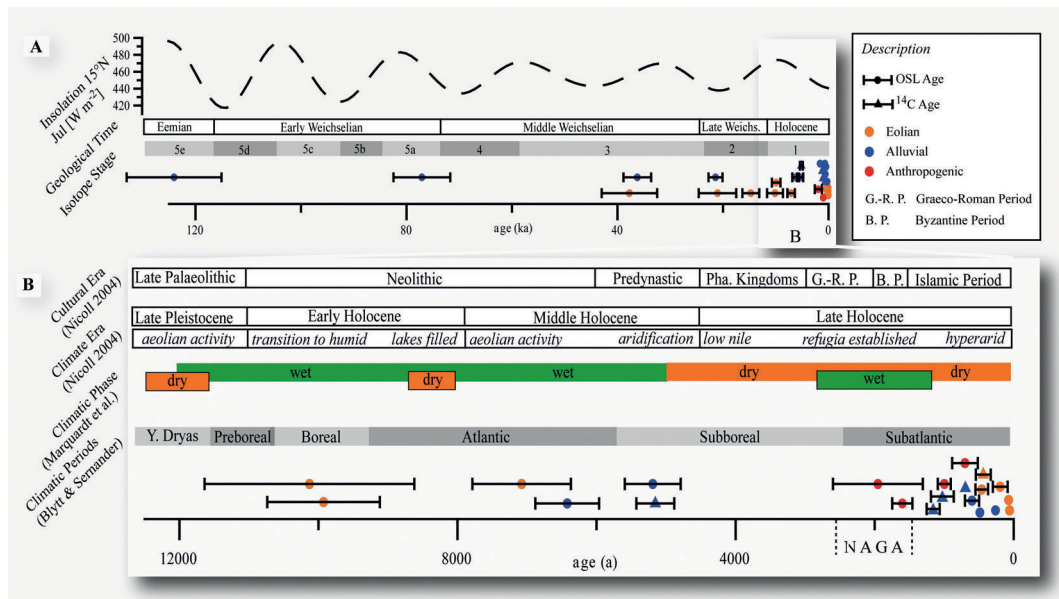


Fig. 5 | The regional scale contextualization. Timescale of all age determinations, including their standard deviation and type. A: The entire timeline of all age determinations with the summer July insolation at 15° N being responsible for the monsoon intensity and therefore one of the main triggers of wetter conditions. B: The Holocene timeline with the cultural and environmental context, based on various sources. J. Berking.

triggers of the onset and strength of the monsoon system over NE Africa (Fig. 5A).⁴⁸ Therefore our correlation of the regional environmental development with the regional and superregional climatic, environmental or cultural phases is weak (Fig. 5A–B).

As stated by Schütt and Krause,⁴⁹ the proxy data revealed by fragmentary chronostratigraphies are not valid for a broader paleoenvironmental comparison because the proxy data comprise information on different depositional and erosional conditions and might be affected by time-lags of the onsets or reactions of the system to environmental changes. Satisfactory results are likely to be obtained by distinguishing between these effects and by comparing the proxy data (indicating system reactions) with paleoclimatic data based on hindcast modeling (showing system impulses triggering the system reactions) which could be part of future work.⁵⁰

6.2 The Timeframe of Eolian Depositions

The dunes around Naga correspond to primary dunes, whereas drift sands or moving dunes do not occur at Naga nowadays.⁵¹ In general, the formation of primary dunes is controlled by the availability and mobility of reworked sediments and vegetation or a barrier to stabilize the dune. The dunes deposited on the northern and southern slopes of Gebel Naga show comparable material properties due to their homogenous grain size distributions, their geochemical composition and their hydraulic conductivity. However, their colors differ: the dune sands are light yellowish along the northern slope (often termed “erg sands”), and red and reddish-brown on the southern slope (often termed “fossil” or “Qoz dunes”).⁵² Their ages document that active dune deposition, corresponding

48 Sirocko et al. 2007.

49 Schütt and Krause 2009.

50 Schütt and Krause 2009.

51 Wiggs 2001.

52 Grove and Warren 1968; Salzwedel 1997.

to eolian activity, occurred during the Last Glacial (MIS 2). It can be assumed that this eolian activity corresponds to the hyperarid *Kanemien* which characterized the Sahara and its southern margins from the Last Glacial Maximum until approximately 12 ka BP and coincided with a dune advance into ambient regions of the present Sahel.⁵³ No eolian deposits corresponding to the early and middle Holocene were detected, indicating the lack of active dune dynamics during this period.

Most of the relevant ages reported for the region also point to Holocene or late Pleistocene ages, but either they were not directly dated (because OSL techniques evolved later: Grove & Warren; Gläser; Salzwedel)⁵⁴ or they are associated with the formation of paleosoil sequences⁵⁵ or exposed limnic facies, directly pointing to different environmental settings.⁵⁶

Two single ages from the late Holocene point directly to a Meroitic phase: Sample D14 (1.6 ± 0.14 ka), an eolian sand sample obtained from a trench in the “Great Hafir” Basin (120cm depth), represents the post-Meroitic siltation of the Basin. Sample D15 (1.95 ± 0.64 ka) was extracted from sand deposits underlying a burial mound of the cemetery northeast of Naga (Fig. 4). It remains unclear whether this increased eolian dynamics in the late Holocene was caused by diminished vegetation cover due to (a) continuing aridization or (b) increased human impact—thus indicating early desertification processes.

6.3 The Timeframe of Fluvial Deposition

The landscape around Naga during the late Quaternary was highly dynamic in respect of fluvial processes. For instance, the lowest and oldest wadi sediments extracted from the closed tube drillings point to an Eemian age (D28, core Naga 03, 587cm depth). Overlying discontinuous sediments of various phases at different depths apparently include several hiatus. The extracted sediments cover the whole last interglacial cycle with humid and warm conditions similar to those during the African Humid Period in the early Holocene Optimum.⁵⁷ However, it is not possible to draw broader environmental conclusions on the basis of such a single sample. The drilling location and the present-day fluvial dynamics in the Wadi Awatib suggest that the channel bed was also anastomizing in the past, and was thus characterized by continuous deposition and relocation of river bed material coinciding with persistent channel dislocation.⁵⁸ In consequence, continuous, undisturbed sediment sequences cannot be expected in such a location.⁵⁹ Carbonate precipitation at the base of core Naga 03 possibly indicates a temporarily higher groundwater level, allowing ascending groundwater movement and leading to precipitation of CaCO₃-minerals (and calcareous aggregates found ubiquitous in depth from 450cm downwards) in the groundwater-unsaturated soil zone. While the present groundwater level is about ~75m below the surface,⁶⁰ calcrete precipitations at ~450cm depth cannot be classified chronologically as they require seasonally changing levels of the near-surface groundwater table or the water-saturated soil zone. This can be expected to occur periodically during flooding of the Wadi Awatib as a consequence of the monsoonal rainfalls.

Age determinations of Naga 02 span the middle to late Holocene and reveal time ranges of several millennia within a few centimeters of the alluvial samples. This implies

53 Grunert 1988.

54 Grove and Warren 1968; Gläser 1987; Salzwedel 1997.

55 Felix-Henningsen 2000.

56 Pachur and Hoelzmann 2000.

57 Sirocko et al. 2007.

58 Morisawa 1968.

59 Morisawa 1968.

60 Edmunds et al. 1992.

repeated hiatus, and consequently the data are hardly appropriate for the reconstruction of landscape and morphodynamics during the Meroitic settlement phase (Fig. 4 and Tab. 4)

6.4 The Timeframe of Mass Movements

OSL dating of the unconsolidated material covering the mass movements at the base of the steep slope of the Gebel Naga yields an age between 70 and 36 ka, corresponding to MIS 5a to MIS 3 and gives a minimum age of the underlying mass movements (Tab. 2). The last phase of reported mass movement activity along the Saharan escarpments has been roughly dated to the late Quaternary.⁶¹ Corresponding to the steep slopes of the escarpment area at Gebel Naga, mass movements are a characteristic shaping element, representing an escarpment retreat.⁶²

6.5 The Meroitic Phase

During the Meroitic settlement phase between 400 BCE and 400 CE, the landscape around Naga was similar to today's. This is documented by the age determination of the upper layers of several dunes indicating early- and mid-Holocene ages, pointing to persistent dune complexes on both the windward and leeward sides of Gebel Naga (D19–23). The samples extracted from the drillings in the alluvial sediments of Wadi Awatib reveal deposits throughout the Meroitic settlement phase and account for persistent alluvial sedimentation at least since Late Pleistocene times (D7,17,18,24,28). Evidence of the settlement phase and a verifying check on the quality of our OSL data are provided by the direct dating of the quartz sands corresponding to the presumed Meroitic phase at the northern cemetery (D15). The continuous silting-up with slackwater and eolian deposits in the Hafir basin (D4,8,9,10,15) also directly points to post-Meroitic times. Also in good agreement are the drift sands (D11) that covered the Amun temple after the abandonment of the city until its excavation in recent years (cf. Fig. 4 and Tab. 3).⁶³

7 Conclusions

The age determinations of fluvial, eolian and mass movement deposits in the vicinity of Naga show a wide range from very young ages (several decades) to very old ages (into the Eemian). The relevant geoarchaeological time slice for the landscape reconstruction during the Meroitic settlement phase from roughly 400 BCE to 400 CE is displayed in only a few age determinations. Satisfactory results are likely to be obtained by distinguishing between short and long term environmental changes and by comparing paleoenvironmental reconstructions based on proxy data with paleoclimate data based on hindcast modeling (showing system impulses triggering the system reactions), which is part of ongoing work. In summary, geoarchaeological investigations in comparable highly dynamic environments such as drylands or desert margins and the expectation of landscape reconstructions for such distinct time slices offer challenging possibilities. The direct dating of eolian sediments revealed very good results, at least on late Quaternary timescales, but also shows the possibilities in respect of the exact and non-destructive age determination of sediments like sample D15 pointing exactly to the presumed Meroitic construction time.

61 Grunert 1979.

62 Berking and Schütt 2011; Busche 1998.

63 Berking et al. (Forthcoming).

Bibliography

Aktar-Schuster and Mensching 1993

M. Aktar-Schuster and H.G. Mensching. "Desertification in the Butana". *GeoJournal* 31.1 (1993), 41–50.

Berking, Beckers, and Schütt 2010

J. Berking, B. Beckers, and B. Schütt. "Runoff in Two Semi-arid Watersheds in a Geoarcheological Context — a Case Study of Naga, Sudan and Resafa, Syria". *Geoarcheology* 25.6 (2010), 815–836.

Berking and Schütt 2011

J. Berking and B. Schütt. "Late Quaternary Morphodynamics in the Area of the Meroitic Settlement of Naga, Central Sudan". *Zeitschrift für Geomorphologie, Supplementbände Volume 55 Supplementary Issue 3* (2011), 1–24.

Berking et al. (Forthcoming)

J. Berking et al. "Geoarchaeological Methods for Landscape Reconstruction at the Excavation Site of Naga, Central Sudan". *Die Erde*. Forthcoming.

Busche 1998

D. Busche. "Das Djado-Plateau: Genese einer zentralsaharischen Schichtstufen-Landschaft". In *Deutscher Geographentag München 46*. Ed. by H. Becker and W. Hütteroth. 1998, 326–331.

Bussert 1998

R. Bussert. "Die Entwicklung intrakontinentaler Becken im Nordsudan". *Berliner Geowissenschaftliche Abhandlungen A* (1998), 196.

Edmunds et al. 1992

M. Edmunds et al. "Sources of Recharge at Abu Delaig, Sudan". *Journal of Hydrology* 131 (February 1992): *Issues 1–4*, 1–24.

Eriksson, Olley, and Payton 2000

M. Eriksson, J.M. Olley, and R.W. Payton. "Soil erosion history in central Tanzania based on OSL dating of colluvial and alluvial hillslope deposits". *Geomorphology* 36 (December 2000): *Issues 1–2*, 107–128.

Felix-Henningsen 2000

P. Felix-Henningsen. "Paleosols on Pleistocene Dunes as Indicators of Paleo-Monsoon Events in the Sahara of East Niger". *CATENA* 41 (September 2000): *Issues 1–3*, 43–60.

Fuchs 2006

M. Fuchs. "Mensch und Umwelt in der Antike Südgrichenlands". *Geographische Rundschau* 4 (2006), 4–11.

Gabriel 1997

B. Gabriel. "Zur quartären Landschaftsentwicklung der nördlichen Butana (Sudan)". *Mitteilungen der Sudanarchäologische Gesellschaft zu Berlin* 7 (1997), 23–30.

Gladfelter 1977

B. Gladfelter. "Geoarchaeology. The Geomorphologist and Archaeology". *American Antiquity* 42 (1977), 519–538.

Gläser 1987

B. Gläser. *Altdünen und Limite in der nordlichen Republik Sudan als morphogenetisch-paläoklimatologische Anzeiger. Untersuchungen zur junquarteren morphologischen Sequenz eines Regionalkomplexes*. Hamburg: Akademie der Wissenschaften in Göttingen, 1987.

Grove and Warren 1968

A.T. Grove and A. Warren. "Quaternary Landforms and Climate on the South Side of the Sahara". *The Geographical Journal* 134 (1968), 194–208.

Grunert 1979

J. Grunert. "Fossil Landslides in the Central Sahara". In *Palaeoecology of Africa 11*. Ed. by E.M. van Zinderen Bakker. Cape Town: Balkema, 1979, 47–49.

Grunert 1988

J. Grunert. "Klima- und Landschaftsentwicklung in Ost-Niger während des Jungpleistozäns und Holozäns". *Würzburger Geogr. Arb.* 69 (1988), 289–304.

Hinkel 1991

M. Hinkel. "Hafire im antiken Sudan". *Zeitschrift für ägyptische Sprache und Altertumskunde* 118 (1991), 32–48.

Hoelzmann et al. 2004

Philipp Hoelzmann et al. "Palaeoenvironmental Changes in the Arid and Subarid Belt (Sahara-Sahel-Arabian Peninsula) from 150 kyr to Present". In *Past Climate Variability through Europe and Africa*. Ed. by R.W. Batterbee, F. Gasse, and C.E. Stickley. Dordrecht et al.: Springer, 2004, 219–256.

Kleinschroth 1984

A. Kleinschroth. "Wasserreservoirs im Sudan aus der Zeit der Antike". *Mitteilungen aus Hydraulik und Gewässerkunde der TUM* 41 (1984), 75–106.

Kleinschroth 1986

A. Kleinschroth. "Die Verwendung des Hafirs im meroitischen Reich". *Beiträge zur Sudanforschung* 1 (1986), 79–96.

Klitzsch 1970

E. Klitzsch. "Die Strukturgeschichte der Zentralsahara. Neue Erkenntnisse zum Bau und zur Paläogeographie eines Tafellandes". *Geologische Rundschau* 59 (1970), 459–527.

Kröper 2006–2007

K. Kröper. "The End of the Amun-Temple and Beginning of Temple 200 – C14 Dates from Naga". *Cripel* 26 (2006–2007), 231–242.

Kuper and Kroepelin 2006

R. Kuper and S. Kroepelin. "Climate-Controlled Holocene Occupation in the Sahara: Motor of Africa's Evolution". *Science* 313 (2006), 803–807.

Leopold, Wolman, and Miller 1964

L.B. Leopold, M.G. Wolman, and J.P. Miller. *Fluvial Processes in Geomorphology*. San Francisco: Freeman, 1964.

Lian and Roberts 2006

O. Lian and R. Roberts. "Dating the Quaternary: Progress in Luminescence Dating of Sediments". *Quaternary Science Reviews* 25 (2006), 2449–2468.

Marquardt, Krause, and Schütt (In preparation)

N. Marquardt, J. Krause, and B. Schütt. "Late Quaternary Spatiotemporal Analysis of the Palaeoclimate of North Africa and the Near East Based on Proxy-Data". *Quaternary Science Reviews*. In preparation.

Morisawa 1968

M. Morisawa. *Streams – their Dynamics and Morphology*. New York: McGraw Hill, 1968.

Murray and Wintle 2000

A. Murray and A. Wintle. "Luminescence Dating of Quartz Using an Improved Single-Aliquot Regenerative-Dose Protocol". *Radiation Measurements* 32 (2000), 57–73.

Nicoll 2004

K. Nicoll. "Recent Environmental Change and Prehistoric Human Activity in Egypt and Northern Sudan". *Quaternary Science Reviews* 23 (2004), 561–580.

Pachur and Hoelzmann 2000

H.-J. Pachur and P. Hoelzmann. "Late Quaternary Palaeoecology and Palaeoclimates of the Eastern Sahara". *Journal of African Earth Sciences* 30.4 (2000), 929–939.

Pflaumbaum, Pörtge, and Mensching 1990

H. Pflaumbaum, K. Pörtge, and H. Mensching. "Hydrologische Steuerungsfaktoren morphologischer Prozesse in der Nil-Provinz (Rep. Sudan)". *Geoökodynamik* 11.2/3 (1990), 241–256.

Salzwedel 1997

U. Salzwedel. "Bildungsbedingungen von Goz- und Ergsand". In *Forschungen im Sudan*. Ed. by K.-H. Pörtge. Erfurter geographische Studien 5. Erfurt: Inst. für Geographie, 1997, 33–48.

Scheibner 2004

T. Scheibner. "Neue Erkenntnisse zur Wasserversorgung von Musawwarat es Sufra (I). Das übergeordnete Wasserversorgungssystem — Teil I: Wassergewinnung und -speicherung". *Mitteilungen der Sudanarchäologischen Gesellschaft zu Berlin e. V.* 15 (2004), 39–65.

Schütt and Krause 2009

B. Schütt and J. Krause. "Comparison of Proxy-Based Palaeoenvironmental Reconstructions and Hindcast-Modelled Annual Precipitation. A Review of Holocene Palaeoenvironmental Research in the Central Sahara". *Palaeoecology of Africa* 29 (2009), 23–37.

Sirocko et al. 2007

F. Sirocko et al. *The Climate of Past Interglacials*. Ed. by J. van der Meer. Developments in Quaternary Science. Amsterdam: Elsevier, 2007.

Stuiver, Reimer, and Braziunas 1998

M. Stuiver, P. Reimer, and T. Braziunas. “High-Precision Radiocarbon Age Calibration for Terrestrial and Marine Samples”. *Radiocarbon* 40.3 (1998), 1127–1151.

Wiggs 2001

G. Wiggs. “Desert Dune Processes and Dynamics”. *Progress in Physical Geography* 25.1 (2001), 53–79.

Wintle and Murray 2006

A. Wintle and A. Murray. “A Review of Quartz Optically Stimulated Luminescence Characteristics and their Relevance in Single-Aliquot Regeneration Dating Protocols”. *Radiation Measurements* 41.4 (2006), 369–391.

Zech and Hintermeier-Erhard 2002

W. Zech and G. Hintermeier-Erhard. *Böden der Welt. Ein Bildatlas*. Heidelberg et al.: Spektrum Akademischer Verlag, 2002.

Digital Resource

GLOBALSOD

National Climatic Data Center, ed. *Global Historical Climatology Network–Monthly*. <http://iridl.ldeo.columbia.edu/SOURCES/.NOAA/.NCDC/.DAILY/.GLOBALSOD/>.

Jonas Berking

2001–2007 Studied Geography, Chemistry, Geology and Meteorology at the Freie Universität Berlin; 2003–2004 Exchange student at University of Wroclaw, Poland; 2007 Diploma Degree (MSc equivalent) at Freie Universität Berlin; 2011 Dissertation at Freie Universität Berlin (Thesis is published online: http://www.diss.fu-berlin.de/diss/receive/FUDISS_thesis_000000034747?lang=en). Research interests: Geoarchaeology (Northern Africa and Central Asia); Quaternary landscape evolution and climate history; Hydrology and water harvesting strategies in drylands.

2001–2007 Studium der Geographie, Chemie, Geologie und Meteorologie an der Freien Universität Berlin; 2003–2004 Auslandsemester an der Universität Wroclaw, Polen; 2007 Geographie-Diplom an der Freien Universität Berlin; 2011 Promotion an der Freien Universität Berlin (Online-Publikation der Arbeit unter http://www.diss.fu-berlin.de/diss/receive/FUDISS_thesis_000000034747?lang=en). Forschungsinteressen: Geoarchäologie (Nordafrika, Zentralasien); Quartäre Landschaftsentwicklung und Klimageschichte; Wassereinzugsgebiete und Geschichte der Wassernutzung in Trockenräumen.

Jonas Berking
Freie Universität Berlin
Department of Earth Sciences, Physical Geography
Malteserstraße 74–100
12249 Berlin, Germany

and

Leibniz Institute for Applied Geosciences
Section S3: Geochronology and Isotope Hydrology
Stilleweg 2
30655 Hannover, Germany
Jonas.Berking@Fu-Berlin.de

Brigitta Schütt

2000–2001, Assistant Professor in Physical Geography, University of Trier; 2002, Substitute Extraordinary Professor in Physical Geography, Universität Bonn; since 2002 Professor, Institute of Geographical Sciences, Freie Universität Berlin, and since 2010 Vice President for Science at Freie Universität Berlin. Research interests: Past and present soil erosion, Late-Quaternary Paleoenvironments, Paleohydrology, Past and Present Morphodynamics, Drylands, Watershed Management

2000–2001, Assistant Professor in Physischer Geographie, Universität Trier; 2002, Vertretung der Professur für Physische Geographie, Universität Bonn; seit Oktober 2002, Professur für Physische Geographie an der Freien Universität Berlin; seit 2010 Vizepräsidentin der Freien Universität Berlin. Arbeits- und Themenschwerpunkte: Bodenerosion, jungquartäres Paläoklima, Paläohydrologie, Morphodynamik, Trockengebietsmorphologie, Watershed Management.

Brigitta Schütt
Freie Universität Berlin
Department of Earth Sciences, Physical Geography
Malteserstraße 74–100
12249 Berlin, Germany
Brigitta.Schütt@Fu-Berlin.de